LASER INTERFEROMETER GRAVITATIONAL WAVE OBSERVATORY

LIGO Laboratory / LIGO Scientific Collaboration

LIGO- T070001-00-R 12/18/2006

Suspension Thermal Noise in Initial and Enhanced LIGO

Gregory Harry, Steve Penn, Andri Gretrasson, Joe Betzweiser, Sam Waldman, Rai Weiss

Distribution of this document:
LIGO Science Collaboration

This is an internal working note
of the LIGO Project.

California Institute of Technology
LIGO Project - MS 18-34
1200 E. California Blvd.
Pasadena, CA 91125
Phone (626) 395-2129
Fax (626) 304-9834
E-mail: info@ligo.caltech.edu

Massachusetts Institute of Technology
LIGO Project - NW17-161
175 Albany St
Cambridge, MA 02139
Phone (617) 253-4824
Fax (617) 253-7014
E-mail: info@ligo.mit.edu

LIGO Hanford Observatory
P.O. Box 1970
Mail Stop S9-02
Richland WA 99352
Phone 509-372-8106
Fax 509-372-8137

LIGO Livingston Observatory
P.O. Box 940
Livingston, LA 70754
Phone 225-686-3100
Fax 225-686-7189

http://www.ligo.caltech.edu/

1 Overview

1.1 Theory of Suspension Thermal Noise

Thermal noise arises from loss in a system in thermal equilibrium according to the Fluctuation-Dissipation Theorem [1]. In a mechanical system like the mirrors and suspensions in LIGO, mechanical loss (friction) provides the source of mechanical thermal noise. Mechanical loss can come from many sources, rubbing friction, interaction with air, eddy current damping, etc. but internal friction, a material rubbing against itself, is the only source that can not be eliminated with good design. Ideally, thermal noise from internal friction would be the limiting noise source in the LIGO band where thermal noise dominates.

Thermal noise from the LIGO suspension wires can be expressed as [2]

$$S_x(f) = 4\, k_B\, T\, g\, d/(M\,(2\,\pi f)^2)\,\sqrt{(Y/(16\,\sigma))}\,\phi, \tag{1}$$

where $S_x(f)$ is the position noise spectral density, k_B is Boltzmann's constant, T is the temperature, g is the acceleration due to gravity, d is the thickness of the suspension wire, M is the mass of the test mass, Y is the Young's modulus of the wire, σ is the stress in the wire, and ϕ is the loss angle of the wire material. The loss angle is what characterizes the internal friction of the wire material, and is given by

$$\phi = Im[Y]/Re[Y]. \tag{2}$$

The other parameters in Eq. (1) are known or easily measured for the LIGO suspensions, so determining the loss angle ϕ becomes the primary goal when trying to predict the suspension thermal noise. In general, ϕ is a function of frequency, so determining the frequency dependence of the internal friction is also necessary for predicting suspension thermal noise.

Suspension thermal noise was expected to be the limiting noise source in initial LIGO in the approximate frequency band 40 Hz – 150 Hz [3], as seen in Figure 1. The SRD assumed a viscous model of internal friction for the steel wires of the suspension. Viscous damping would mean that the loss angle would be linear in frequency. This is typical of mechanical loss from objects moving through a dense fluid, like air at atmospheric pressure, but is not typical of internal friction from metals where a frequency independent loss angle, known as structural damping, is more typical [4]. Suspension thermal noise from structural damping would have a steeper slope than noise from viscous damping.

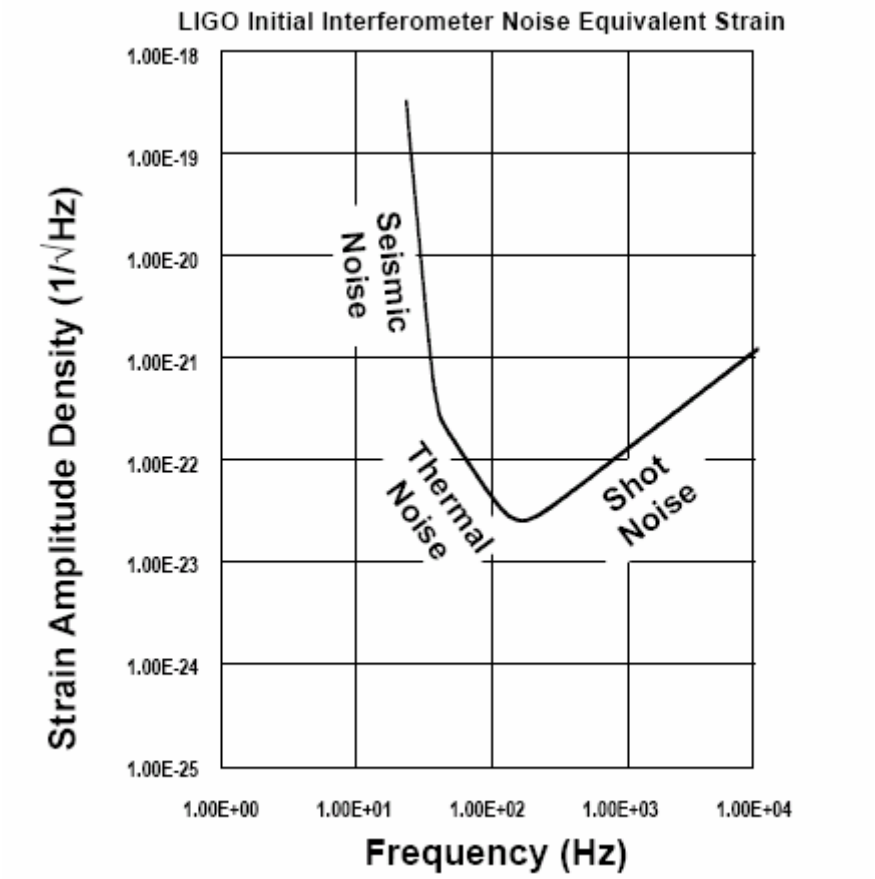

Figure 1. – Initial LIGO noise as predicted by the Science Requirements Document (SRD).

1.2 Measurement of Mechanical Loss

The usual method for determing ϕ is by measuring the quality factor of mechanical modal resonances. Energy loss during a modal oscillation is limited by internal friction, just as thermal noise is. If the only restoring force on the system is due to the elasticity of the material, internal friction and modal quality factor are related by

$$\phi(f_0) = 1/Q, \tag{3}$$

where f_0 is the frequency of the measured mode and Q is its quality factor. By measuring Q's at multiple modes with different frequencies, the frequency dependence of the internal friction can be explored.

There are different mechanisms that can give rise to mechanical loss. Internal friction is one of the most difficult to predict, and because it is often dominant in relevant frequency bands, it usually

has be measured. One important loss mechanism can be predicted very accurately. This is thermoelastic damping, which occurs when contractions in the material give rise to heat that flows to regions that are colder due to rarefactions. If the frequency of the contractions is close to the reciprocal of the time it takes heat to flow between the hot and cold spots, thermoelastic damping can be an important loss mechanism. The ϕ for thermoelastic damping can be found from

$$\phi(f) = Y\,\alpha^2\,T/C\,\gamma f/(1+\gamma^2 f^2) \tag{4}$$

where

$$\gamma = 2\,\pi/13.55\,C\,d^2/\kappa \tag{5}$$

for a fiber geometry, and T is the temperature, C is the heat capacity per unit volume, d is the fiber thickness, and κ is the thermal conductivity.

The suspensions of the initial LIGO mirrors are not a system where the restoring force is due solely to the wire's elasticity, however. Gravity plays a role (either directly or through tension in the wire), and gravity does not contribute loss as elasticity does. The amount of potential energy from gravity relative to the potential energy due to elasticity, known as the "dissipation dilution", is important to calculate correctly when predicting thermal noise and interpreting modal Q results. The "effective" ϕ is found from

$$\phi_{diluted} = U_{elastic}/U_{total}\;\phi_{elastic}, \tag{6}$$

where $U_{diluted}$ is the total potential energy stored in elastic deformations when the wire bends, either in the motion that couples to the laser as thermal noise or in the modal deformation, U_{total} is the total potential energy in both elastic and gravitational fields, and $\phi_{elastic}$ is the internal friction of the wire material. For the thermal noise case, Eq (1) can be written

$$S_x(f) = 4\,k_B\,T/(M\,(2\,\pi f)^2)\;\phi_{effective}\,, \tag{7}$$

where $\phi_{effective}$ is

$$\phi_{effective} = \phi\;d\sqrt{(Y/16\,\sigma)}. \tag{8}$$

Equation (6) is the appropriate dissipation formula for both thermal noise calculations and for interpreting pendulum mode Q's. In this sense, measuring pendulum mode Q's might seem the most direct way to measure loss for thermal noise predicting. However, there are problems with

measuring and interpreting pendulum mode Q's. First, the decay time of a modal resonance is related to the Q by

$$\tau = Q/(\pi f_0). \tag{9}$$

For Q's of a few million, fairly typical for metal wires supporting LIGO mirrors, at a pendulum mode frequency of about 1 Hz, this leads to decay times of millions of seconds, or weeks, making doing the experiment impractical. There are also problems with measuring Q's of LIGO suspensions at pendulum mode frequencies because the motion of the suspension can couple to modes of the seismic isolation stack. This means an additional type dissipation dilution occurs, although this time rather than coupling in a losses gravity component, a typically more lossy spring from the isolation stack must be included. Finally, pendulum mode Q's give mechanical loss at near 1 Hz, well below the 40-150 Hz band where suspension thermal noise is important to the LIGO noise budget. Any frequency dependence to the mechanical loss will be difficult to measure.

These difficulties lead to the violin mode Q's as the best way to measure mechanical loss in the LIGO suspensions. The dissipation dilution factor for violin modes is given by [5]

$$\phi_{diluted} = 2/l \sqrt{(2\ Y\ I/(M\ g))}\ (1 + 1/(2\ l) \sqrt{(2\ Y\ I/(M\ g))}\ (n\ \pi)^2)\phi, \tag{10}$$

where l is the length of the wire, I is the area moment of inertia, and n is the harmonic number of the violin mode. Using Eqs. (3) and (8), the intrinsic material ϕ of the suspension wire material can be discovered from violin mode Q measurements. Then using Eqs. (5) and (6), the level of suspension thermal noise can be predicted from this ϕ.

2 Q Measurements at the LIGO Sites

The violin mode Q's of the actual suspension wires supporting the test masses at the two LIGO sites have been measured. Two separate measurement techniques, a frequency domain and a time domain, have been used. These measurements were typically of the lowest order violin modes, as well as the higher order modes, including the n=1 and n=2 modes. This gives some data on possible frequency dependence of the loss. Repeatability, amplitude dependence, and dependence on stored optical power was also investigated.

2.1 Frequency Domain Violin Mode Measurements

The lowest order violin modes of the LIGO optics occur near 350 Hz. The exact values are given in Table 1. These values are stable to the 1 millihertz level, but temperature drift leading to changes of wire Young's modulus cause the frequencies to change on the milliHertz level.

Table 1. – Frequencies of the lowest order violin modes in all LIGO test masses. The frequencies typically are not stable to milliHertz. The two sets of values for LHO 4K ITMx represent the modes of the original mirror (on left) and replacement mirror (on right).

Interferometer	Test Mass	Lower Violin Mode	Higher Violin Mode
LLO	ITMx	346.65 Hz	347.04 Hz
	ITMy	346.91 Hz	346.96 Hz
	ETMx	343.09 Hz	343.65 Hz
	ETMy	343.48 Hz	344.42 Hz
LHO 4K	ITMx	347.17 Hz : 347.31 Hz	347.27 Hz : 347.51
	ITMy	347.68 Hz	347.72 Hz
	ETMx	343.41 Hz	344.06 Hz
	ETMy	344.70 Hz	344.82 Hz
LHO 2K	ITMx	348.94 Hz	349.45 Hz
	ITMy	349.19 Hz	349.24 Hz
	ETMx	343.81 Hz	344.05 Hz
	ETMy	343.75 Hz	344.09 Hz

During low noise operation, the violin modes are clearly visible in the LIGO noise spectra, see Figure 2. A spectrum around the modes can be collected where the modes are visible as peaks with widths, typically a frequency resolution around 0.1 mHz. The Q of the mode is related to the width of the peak by

$$Q = f_0/\Delta f \tag{11}$$

where Δf is the peak width when the height is 3dB down from the peak of the amplitude spectral density. Data can then be fit to a Lorentzian and the Q value extracted.

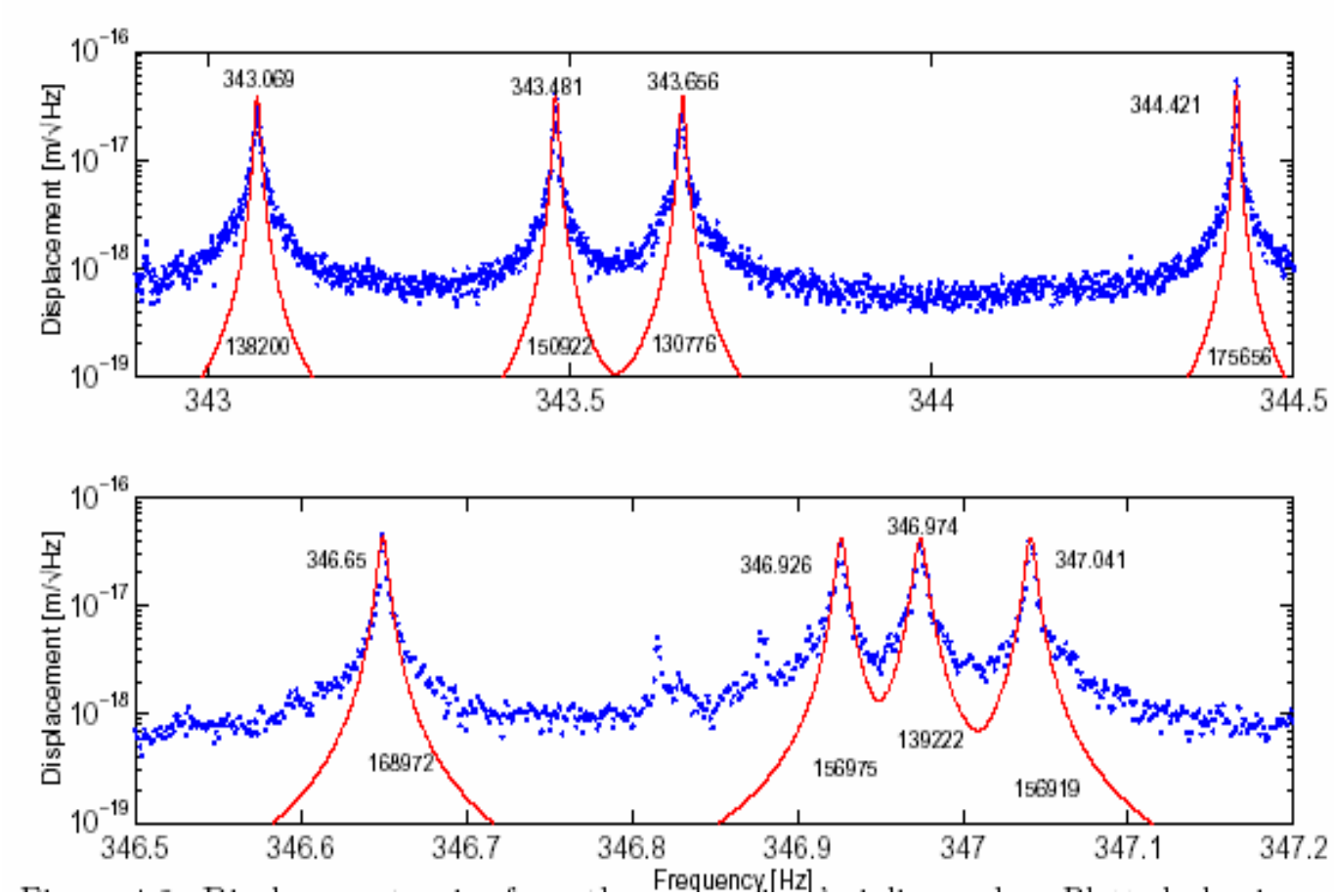

Figure 2. Amplitude spectral density of LIGO Livingston noise around the lowest order violin modes. The numbers near the peak represent the central frequencies, while the lower numbers are the Q's of the modes. Figure from R. Adikari's thesis.

Data was collected and Q's fit for on data from the n=0, n=1, and n=2 violin modes of the LHO 2K and 4K many times, during the same lock stretches as well as differing ones. Typically, no agreement was seen between Q's in any data file, whether it was from the same lock stretch or not. Some data did give the same Q's as other data from the same lock stretch, within the fitting error bars. However, changes in Q by up to a factor of 17 were observed for the same mode within the same lock stretch. It is also noted that the data deviates from the predicted Lorentzian shape before reaching a stable noise floor. As is seen in Fig. 2, the tails of the peaks have a shallower slope than the Lorentzian in the lower part of the peaks.

The radical changes in Q and the peak's deviation from the Lorentzian shape leads to the conclusion that frequency domain fitting is not a reliable way to determine mechanical loss. One possible explanation is that temperature drift causes peak frequency drift that is not negligible during the ringdown time of about 20 minutes. Variation in test mass internal mode frequencies

and their correlation with temperature was studied by Andri Gretarsson with SURF student Briony Horgan [6]. They concluded that the frequencies did track with LVEA temperature; it is possible the violin mode frequencies do as well. However, temperature drift would likely blur the central frequency, not keep a sharp peak but cause shallower slope away from the peak. As seen in Figure 2, the central frequency is well defined and in good agreement with Table 1.

2.2 Time Domain Violin Mode Measurements

2.2.1 Technique

Measuring Q's using the time domain ringdown technique does not suffer (as much) from the problems of the frequency domain technique. Here the violin mode is excited by driving on resonance through one of the OSEM coils until the mode's amplitude is well above the noise. Then the drive is removed, and the mode is allowed to ring freely. Mechanical loss in the system will cause the oscillation to damp away, with a frequency-independent ϕ causing an exponential decay. The amplitude is then fit to the formula

$$X = X_0 \, e^{-t/\tau} \sin(2 \, \pi f_0 \, t + \beta) \tag{12}$$

and the Q of the mode is determined from

$$Q = \pi f_o \, \tau, \tag{13}$$

where τ is the decay time of the mode and β is an arbitrary phase. This technique suffers from the problem that it can not be used during Science Mode and that the ϕ at thermal excitation levels may be different than when the mode is intentionally excited (amplitude dependence). Amplitude dependence can be explored partially by using different amounts of excitation (see below).

2.2.2 Time Domain Q Data

Time domain ringdown data was collected at both sites on many mirrors, wires, and modes. The full data is shown in Table 3.

2.3 Issues in the Time Domain Q Data

2.3.1 Agreement with material loss

Using Eqs. (4) and (10), numerical predictions of expected Q's can be made and compared with the data in Table 3, as long as good estimates of the input parameters are known. The relevant parameters are given in Table 5. Using these values in Eqs. (4) and (10) predictions can be made for measured Q's

$$1/Q(f) \; = \; ((8.0 \; 10^{-6} \; /\mathrm{Hz} \, f) \, / \, (1 + (f \, / \, 228 \; \mathrm{Hz})^2 \,) + \phi) \, / \, 172, \tag{14}$$

where the first term comes from thermoelastic damping and the second is the wire's material loss, while the overall factor of 172 comes from dissipation dilution. Using the mode frequencies and a material ϕ of 1.7 10^{-4} obtained on free wire measurements at Hobart and William Smith Colleges and described below in Section 3.1, the predicted Q for the first three violin modes are

$$\begin{aligned} Q_{pred}\,(350\ \text{Hz}) &= 1.7\ 10^5 \\ Q_{pred}\,(700\ \text{Hz}) &= 2.4\ 10^5 \\ Q_{pred}\,(1050\ \text{Hz}) &= 3.1\ 10^5 \end{aligned} \tag{15}$$

The highest Q's seen for these three modes are $Q_{pred}(350\ \text{Hz}) = 1.65\ 10^5$ on LLO ITMx Higher 1 on March 15, 2004, $Q_{pred}(700\ \text{Hz}) = 1.65\ 10^5$ on LLO ITMx Higher 1 on March 15, 2004, and $Q_{pred}(1050\ \text{Hz}) = 2.61\ 10^5$ on LHO 2K ITMy on Higher 3 on January 29, 2005. Only the first harmonic value is close to the theoretical prediction, and that is a single example amongst many measurements that fall well short of the theory. Clearly excess loss is dominating the loss for many wires on many optics.

Table 4 – Parameters used to fit the measured violin mode Q data for the wire material ϕ. HWS refers to laboratory measurements made at Hobart and William Smith Colleges and are described in full in Section 3.1 below. Handbook refers to Ref. [9].

Parameter	Value	Source
Y - Youngs' Modulus	182 GPa	Direct measurement - HWS
α – Thermal expansion	11.4 10^{-4} /K	Fit to free wire data – HWS
C_m – Specific heat per unit mass	486 J/(kg K)	Handbook
ρ – Mass density	7800.0 kg/m^3	Handbook
κ – Thermal conductivity	37.3 J s/(m K)	Fit to free wire data – HWS
d – Wire diameter	3.05 10^{-4} m	Manufacturer data
l – Wire length	0.44 m	Suspension design
I – Moment of inertia $\pi d^4/64$	4.2 10^{-16} m^4	Calculation
M – Mass	10.5 kg	Optic design

2.3.2 Inconsistency between lock stretches

Another aspect of the data shown in Table 3 is that the Q for a given mode is sometimes but not always inconsistent between different measurements. Examples of differing Q's for the same mode include LHO 4K ETMx Lower 1 on April 5 2006 and April 7 2006, LHO 4K ITMx Lower 1 on June 24, 2005 and April 7, 2006, LLO ITMx Higher 1 on June 3, 2005 and May 16, 2006, and LLO ITMx Lower 1 on May 31, 2005, June 2, 2005, and June 3, 2005. However, within a given lockstretch the modes do often maintain the same Q, see for example LLO ITMy Lower 3 on January 19, 2005, LLO ITMx Lower 1 on June 2, 2005 at 1:45, or LLO ITMx Lower 1 on June 3, 2005 at 3:15.

A comparison of three different ringdowns of mode LLO ITMx Lower 1 from three different lock stretches is shown in Figure 3.

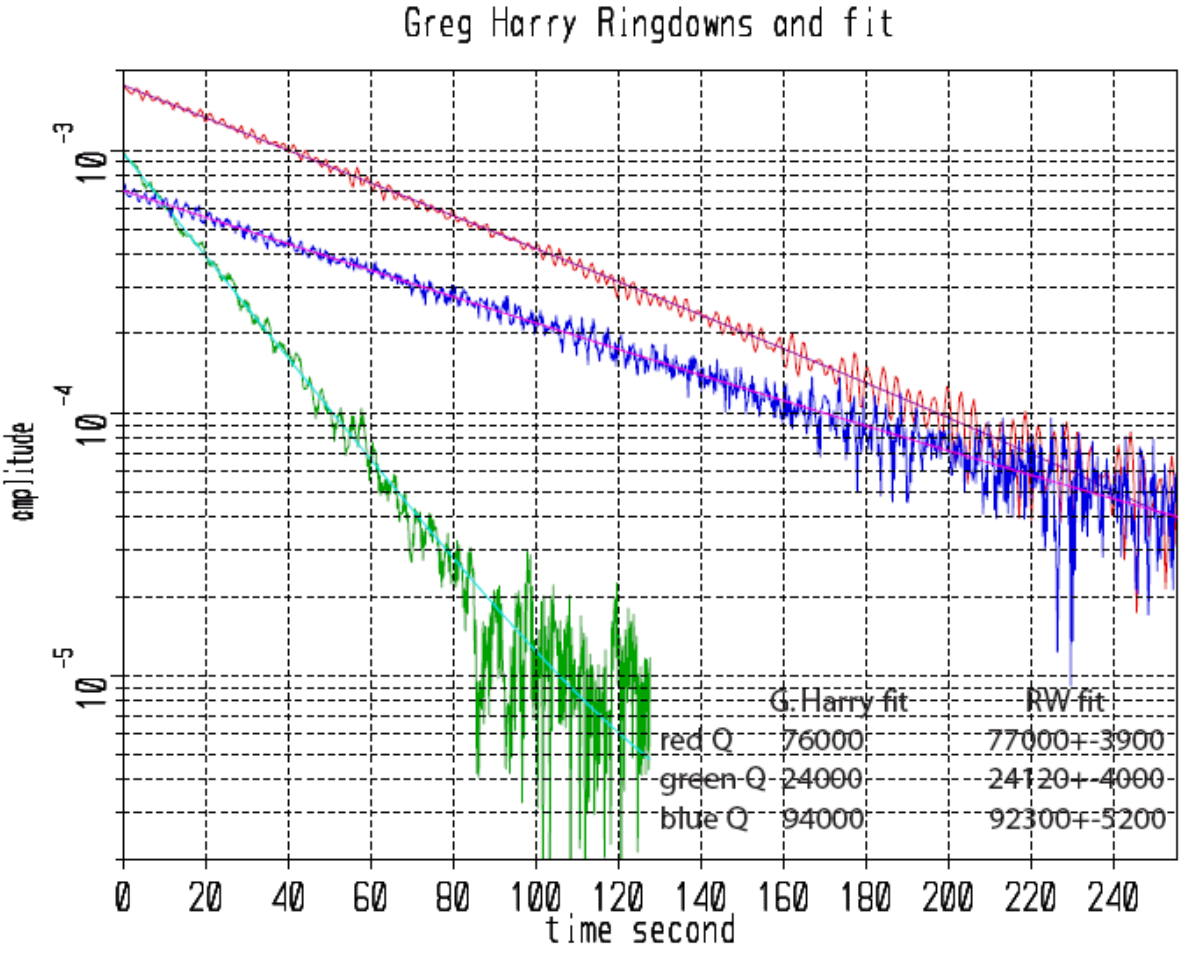

Figure 3. Ringdowns of mode LLO ITMX Lower 1 from three different measurements, along with fits to the data using two different fitting programs.

2.3.3 Possible Causes of Issues and Experiments

There are a number of mechanisms that could cause measured modal Q's to be lower than theory predicts and/or differ between trials. The effects of feedback on the wires, mechanical changes between the wire and the top clamp and/or the wire and the bottom standoff, inaccurate fitting of the data, and temperature drift changing recoil damping with the suspension cage were all suggested as explanations. Feedback and mechanical changes were explored by varying parameters and remeasuring Q's. Problems with fitting were examined using multiple fitting programs, while temperature drift was explored at Embry-Riddle Aeronautical University and is described in Section 3.2.

2.3.3.1 Feedback

Measurement of modal Q's must be done carefully in a system that includes active feedback, and there are many feedback loops operating in the LIGO interferometers. Depending on the phase of the mode and any feedback, measured Q's can be below or above the true thermodynamic value.

The ITM's are not actuated on by the LSC loops, and only have their local ASC loops. The ASC loops have a unity gain frequency around 1 Hz, so it is unlikely they could be interfering with modal Q measurements at the 350 Hz or at higher harmonics. This would leave actuation through the cavity as an optical spring as the only mechanism that could lead to feedback contamination of ITM modes. Such an effect would scale with the amount of power stored in the cavity, so measurements of Q vs optical power would show a clear effect. Data on Q versus power requested into the Mode Cleaner was taken for LLO ITMx Lower 1 on June 3, 2005 at 3:15 and for LLO ITMx Higher 1 on June 3/2005 at 2:20. A graph of both sets of data is shown in Figure 4. Neither show any change in modal Q with optical power.

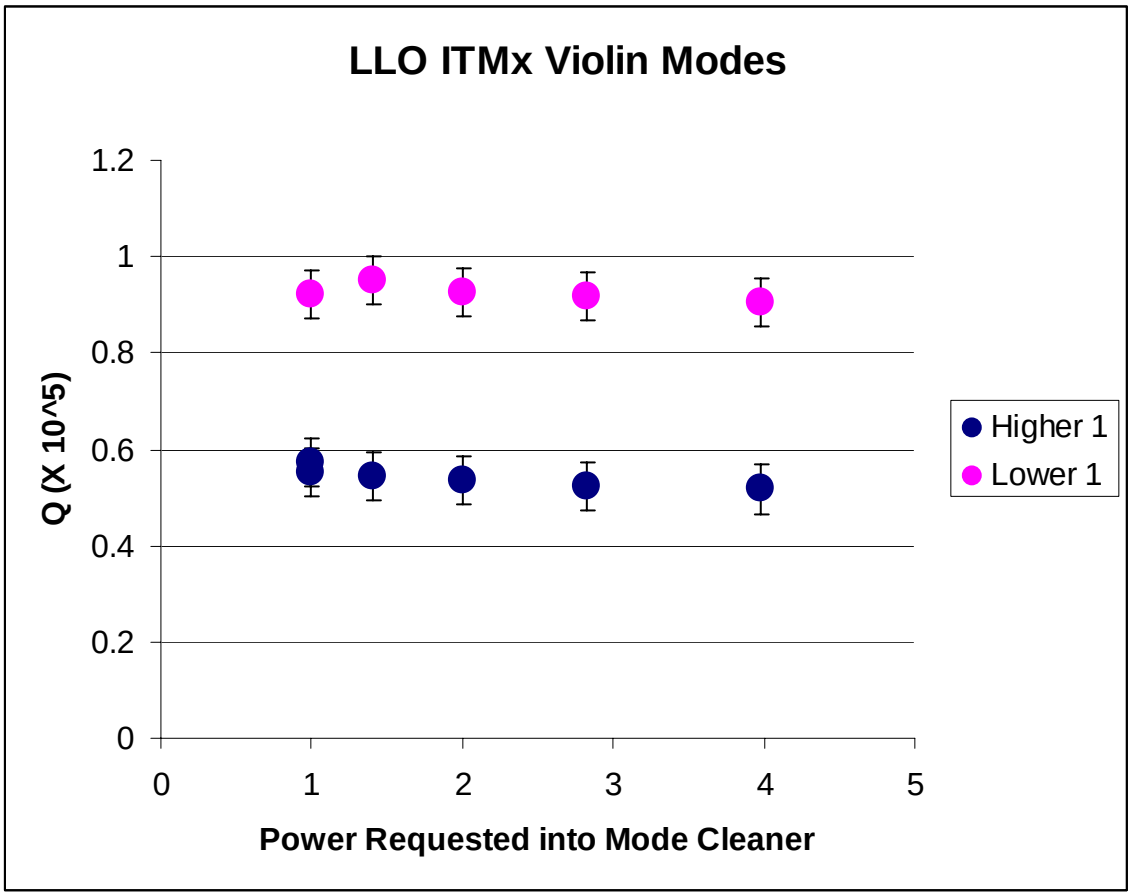

Figure 4. Violin mode Q's for LLO ITMx Higher and Lower 1 as a function of laser power requested into the mode cleaner. Error bars at the 5% level in Q are shown. The lack of response of the modal Q's to optical power indicates feedback through an optical cavity is not affecting the measured mechanical loss.

2.3.3.2 Mechanical Changes

Another possible explanation for the inconsistent Q's is a change in mechanical rubbing friction between either the clamp at the top of the suspension or the standoff at the bottom attached to the optic. This could explain why the Q's are typically consistent within a lockstretch, when the optics move very little, but could change between lockstetches when the process of losing and reacquiring lock allows the mirrors to move by microns relative to the suspension cage.

Data was collected on LLO ITMx Lower 1 on June 3, 2005 at 3:15 as a function of position of the optic relative to the suspension cage. This was affected by moving the optic within the lockstretch by changing the amount of current to coils. Results are shown if Figure 5 and indicate no change within the error bars of the measured Q's. This is a difficult result to interpret, as it could just indicate that at this particular time or for such gentle forces, the wire does not appreciably change its friction with the clamp or standoff.

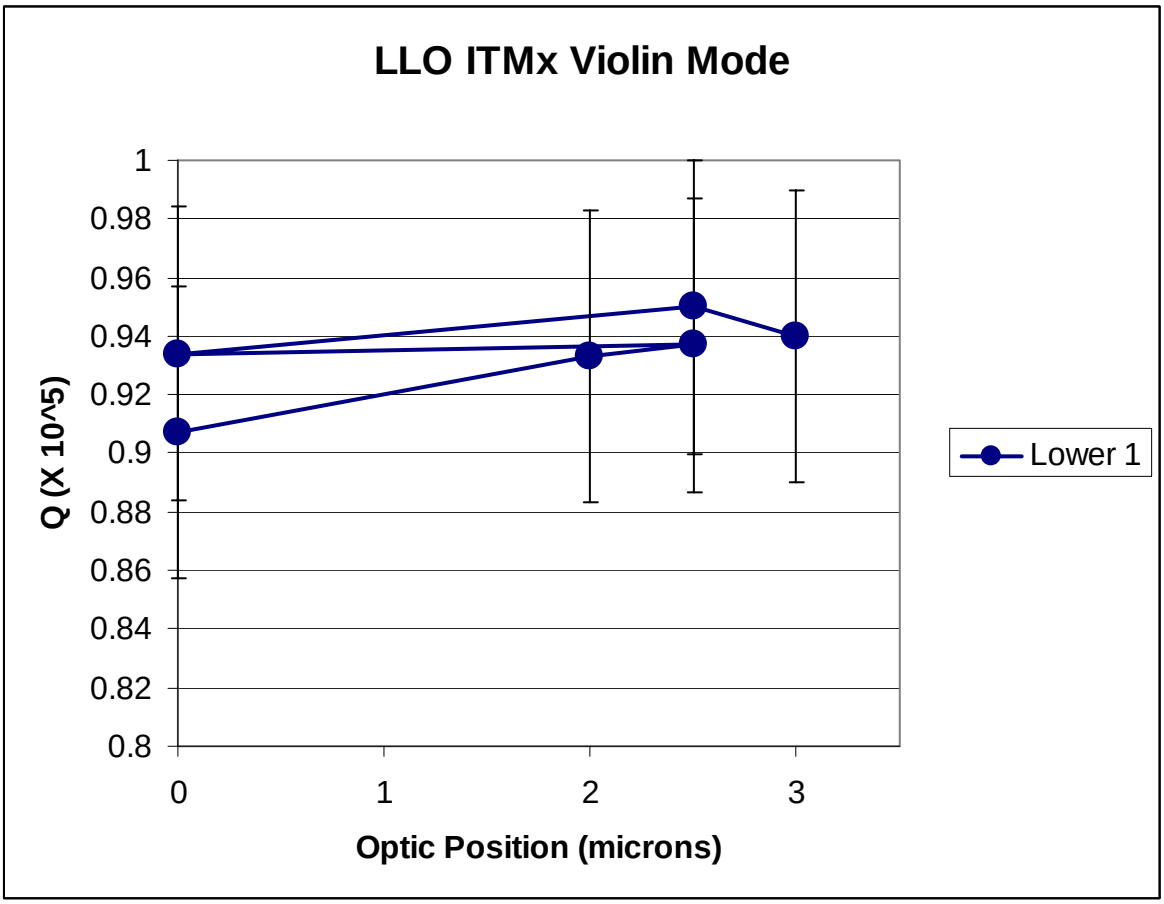

Figure 5. Violin mode Q's for LLO ITMx Lower 1 as a function of optic position. Error bars at the 5% level in Q are shown. The line shows the order in time that the measurements were taken, beginning with the lower point at position 0.

2.3.3.3 Problems with Fitting

Another suggested explanation of the inconsistency of the Q's was possible differences between data fitting routines and/or inconsistencies within a given fitting method. Most of the data in Table 3 was fit for Q using various versions of Qfit, a program by Steve Penn. Qfit is used frequently with Q data from the coating mechanical loss program and other Advanced LIGO thermal noise projects (see Refs. 7 and 8 for examples). Some of the data in Table 3 (in particular, the data from LLO on May 16, 2006 and LHO from April 5 and 7, 2006) was fit using specially written code. Figure 3 shows a comparison of three separate ringdowns fit with independently with Qfit (the G. Harry fit) and other code (RW fit) showing agreement within the error bars. As a test of consistency within QFit, the real and imaginary parts of data from LLO May 31, 2005 and LLO June 2, 2005 were fit separately. Any disagreement between these two fits would indicate that Qfit could be unreliable. Results with individual error bars on shown in Table 4. This data does not support the idea that inconsistencies within Qfit can explain the inconsistent observed Q's.

Table 4 – Modal Q fits for both the real and imaginary parts of the collected data, including error bars from Qfit.

Lock Stretch	Mode	Q of Real Part (X 10^5)	Q of Imaginary Part (X 10^5)
5/31/2005 20:00	ITMy Lower -1	0.890 ± 0.04	0.847 ± 0.04
	ITMy Higher -1	0.90 ± 0.05	1.03 ± 0.3
	ITMy Higher -1	1.03 ± 0.05	1.01 ± 0.05
	ITMy Higher -1	0.97 ± 0.04	1.01 ± 0.05
	ITMy Lower -1	0.73 ± 0.05	0.86 ± 0.05
5/31/2005 22:00	ITMy Lower -1	0.67 ± 0.04	0.71 ± 0.06
	ITMy Higher -1	0.85 ± 0.05	1.08 ± 0.05
	ITMy Higher -1	1.0 ± 0.04	0.86 ± 0.06
5/31/2005 1:00	ITMx Lower -1	0.755 ± 0.003	0.755 ± 0.003
5/31/2005 1:40	ITMx Lower -1	0.759 ± 0.004	0.756 ± 0.003
	ITMx Lower -1	0.758 ± 0.004	0.753 ± 0.004
	ITMx Lower -1	0.885 ± 0.003	0.886 ± 0.003
	ITMx Higher -1	0.838 ± 0.004	0.835 ± 0.004
	ITMx Higher -1	0.862 ± 0.003	0.861 ± 0.003
	ITMx Higher -1	0.918 ± 0.004	0.923 ± 0.004
	ITMx Higher -1	0.778 ± 0.002	0.781 ± 0.002
	ITMy Lower -1	0.719 ± 0.01	0.706 ± 0.001
5/31/2005 1:45	ITMx Lower -1	0.240 ± 0.001	0.241 ± 0.001
	ITMx Lower -1	0.251 ± 0.003	0.246 ± 0.01
	ITMx Lower -1	0.251 ± 0.002	0.249 ± 0.002
	ITMx Higher -1	0.871 ± 0.004	0.848 ± 0.004

2.4 Small Optic Suspension Violin Modes

There have been a few violin mode Q measurements on a small optic in situ in the Hanford 4k. These are of interest for having a higher frequency lowest mode and for using metal, rather than glass, for the standoff material. The two lowest frequency modes of one of the wires on the sm mirror were measured, the results shown in Table 5.

2.5 Limits on Suspension Thermal Noise from Noise Data at the Sites

Fits to sus thermal noise from current LIGO noise, Rayleigh-grams, speculation about other noise sources (Barkhousen, coil driver, charging, etc.)

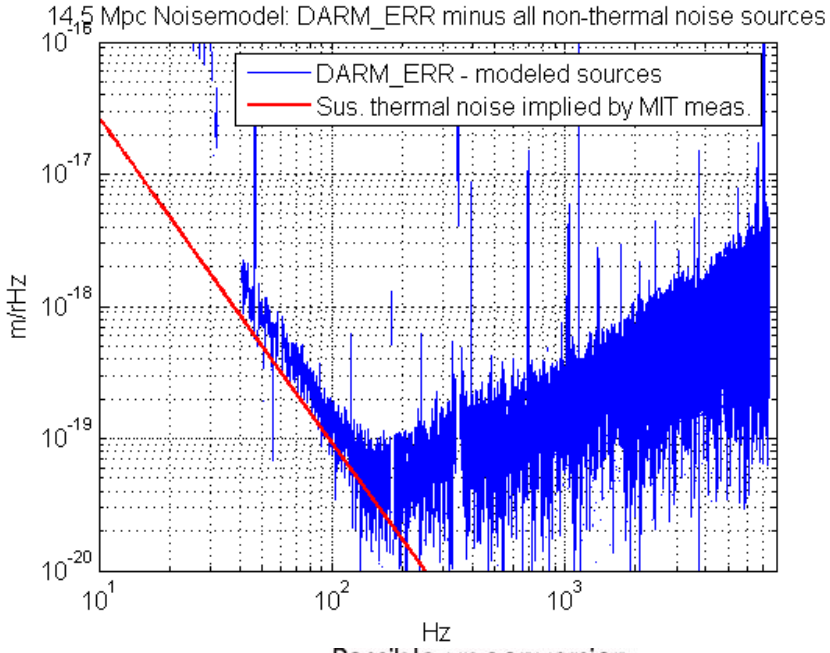

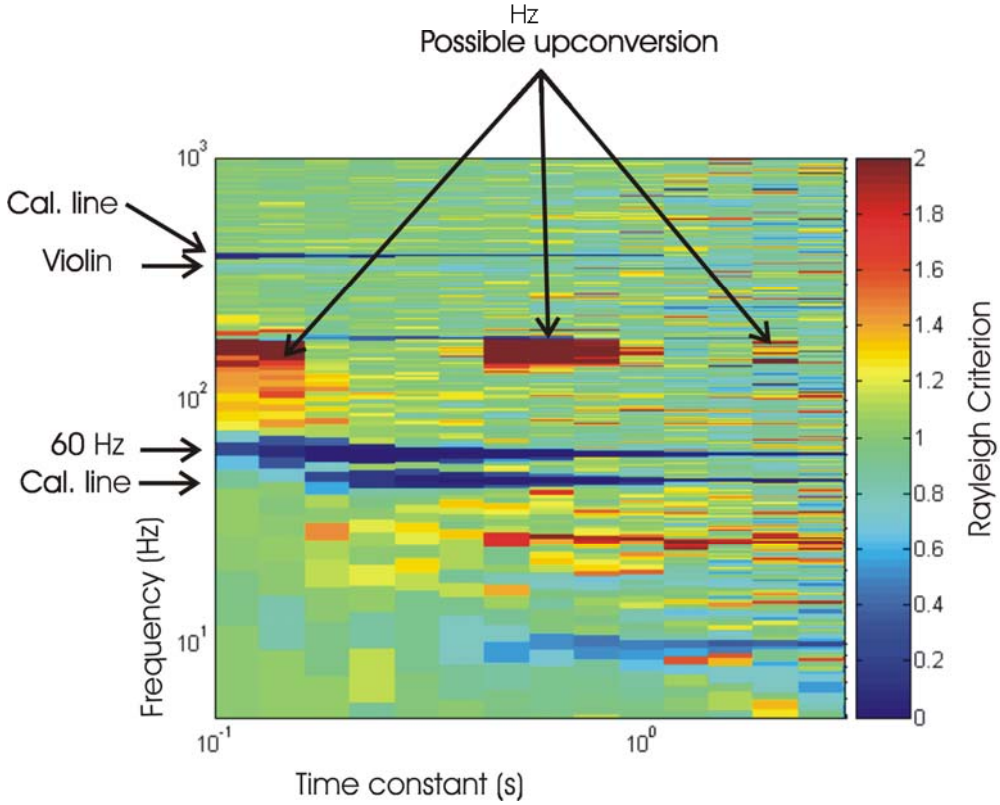


LIGO

3 Laboratory Experiments

3.1 Hobart and William Smith

3.1.1 Free Wire Measurements

Setup, Youngs' modulus tests, measured value of thermoelastic parameters, material limit of phi, comparison with Geppo's numbers

3.1.2 Tensioned Wire Measurements

Collet Results, Virgo clamps

3.2 Embry Riddle Aeronautical University

Cage mode frequencies, comparison with Janeen's values, effect of temperature

3.3 MIT

Setup, results from remachined clamps, Q versus torque, collet results, evidence of galling, Virgo clamp.

Table 5. Violin mode Q's from MIT test setup using a pre-used conventional clamp with temperature as an additional parameter. Temperature in the lab was not controlled, but was changing because of a faulty heating system in the MIT high bay.

Date	Mode	Frequency (Hz)	Q (X 10^5)	Temperature (F)
3/13/06	Left 1 FB	339.820	0.751	72
	Left 1 LR	339.664	1.22	72
	Right 1 LR	338.875	0.743	72
	Right 1 FB	338.984	0.816	72
	Right 1 LR	338.875	0.731	73
	Left 1 LR	339.664	0.639	73
	Left 1 FB	339.820	0.777	73
	Left 1 FB	339.805	0.724	80
	Right 1 LR	338.867	0.753	80
	Right 1 FB	338.977	0.772	80
	Right 1 FB	338.977	0.815	85
	Right 1 LR	338.867	0.730	85
	Left 1 LR	339.648	1.16	85
	Left 1 FB	339.885	0.704	85

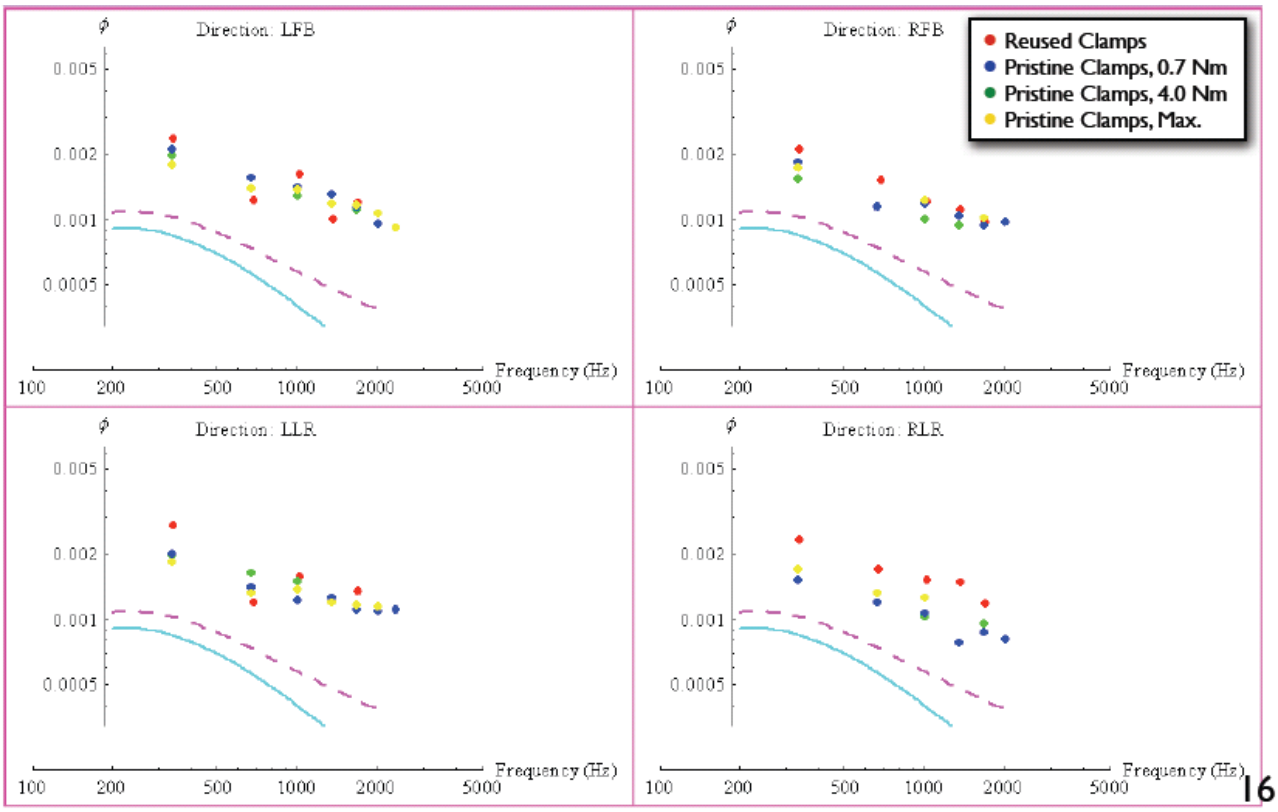
Direction: LFB
Direction: RFB
Direction: LLR
Direction: RLR
Reused Clamps
Pristine Clamps, 0.7 Nm
Pristine Clamps, 4.0 Nm
Pristine Clamps, Max.
0.005
0.002
0.001
0.0005
100
200
500
1000
2000
5000
Frequency (Hz)

16

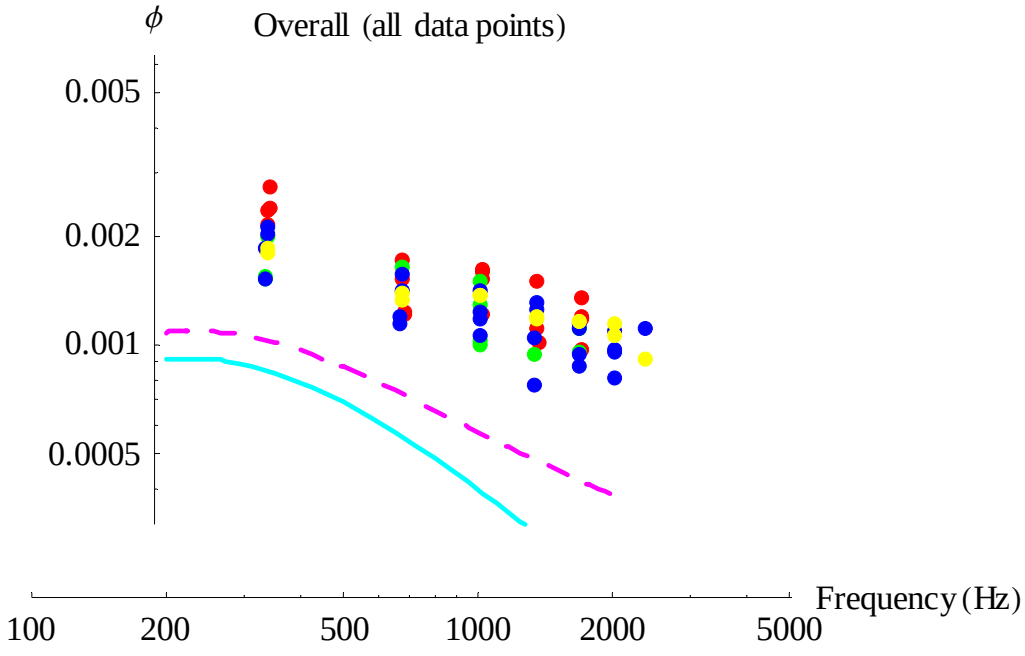
Overall (all data points)
0.005
0.002
0.001
0.0005
100
200
500
1000
2000
5000
Frequency (Hz)

Q's with Virgo clamp compared to LIGO clamps

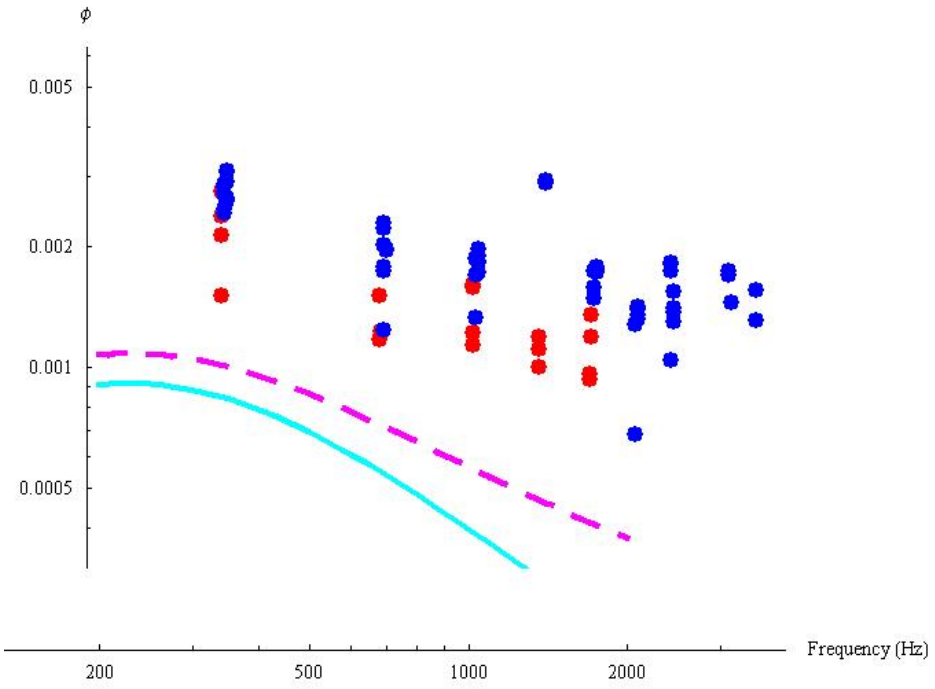

3.4 Future Plans

Ribbons, wires with bobs attached, sapphire clamp, steel standoffs, measure violin mode Qs on small optics at sites (to compare steel standoffs to silica)

Bibliography

1 - H. B. Callen and R. F. Greene, "On a theorem of irreversible thermodynamics", Phys. Rev., **86**, 702-710, (1952).

2- A. M. Gretarsson *et al.*, Phys. Lett. A **270** (2000) 108.

3 – A. Lazzarini and R. Weiss, LIGO Science Requirements Document, LIGO-E950018-02-E.

4- P. R. Saulson, "Thermal noise in mechanical experiments", Phys. Rev. D, **42**, 2437-2445 (1990).

5 – A. Gillespie and F. Raab, "Suspension losses in the pendula of laser interferometer gravitational-wave detectors", Phys. Lett. A **190**, 213-220 (1994).

6 - Andri Gretarsson and Briony Horgan, "Time-Dependence of Test Mass Internal Modes

and Correlations with External Influences", LIGO-T060291-00-R.

7 - G. M. Harry, M. R. Abernathy, A. E. Becerra Toledo, H. Armandula, E. Black, K. Dooley, C. Nwabugwu, A. Villar, D. R. M. Crooks, G. Cagnoli, J. Hough, I. MacLaren, P. Murray, S. Reid, S. Rowan, P. H. Sneddon, M. M. Fejer, R. Route, S. D. Penn, P. Ganau, J.-M. Mackowski, C. Michel,

L. Pinard, A. Remillieux, "Titania-Doped Tantala/Silica Coatings for Gravitational-Wave Detection". *Classical and Quantum Gravity* **24** (2006) 405.

8 - S. D. Penn, A. Ageev, D. Busby, G. M. Harry, A. M. Gretarsson, K. Numata, P. Willems, "Frequency and Surface Dependence of the Mechanical Loss in Fused Silica". *Physics Letters A* **352** (2006) 3.

9 – Handbook that Steve used for wire properties.

Appendices

Table 2 – Measured Q's, using the frequency domain technique, of the first three harmonics of violin modes of both Hanford interferometers over various lock stretches. The mode notation 1l refers to the first violin mode and the lower frequency of the two modes from the given optic.

Interferometer	Lock Stretch	Optic	Mode	Frequency (Hz)	Q (X 10^5)
LHO 4K	10/18/2004	ETMx	Lower -1	343.412	1.6
		ETMx	Higher -1	344.058	1.2
		ETMy	Lower -1	344.714	1.6
		ETMy	Higher -1	344.828	1.6
		ITMx	Lower -1	347.176	1.5
		ITMx	Higher -1	347.266	0.93
		ITMy	Lower -1	347.678	0.59
		ITMy	Higher -1	347.719	0.59
	1/26/2005 14:45	ETMx	Lower -1	343.409	0.70
		ETMx	Higher -1	344.054	1.1
		ETMy	Lower -1	344.711	2.7
		ETMy	Higher -1	344.825	0.89
		ITMx	Lower -1	347.174	1.7
		ITMx	Higher -1	347.264	1.1
		ITMy	Lower -1	347.678	0.81
		ITMy	Higher -1	347.715	0.67
	10/28/2005	ETMx	Lower -2	686.903	1.4
		ETMx	Higher -2	688.274	1.4
		ETMy	Lower -2	689.505	1.4

		ETMy	Higher -2	689.731	2.8
		ITMx	Lower -2	694.271	1.2
		ITMx	Higher -2	694.576	1.3
		ITMy	Lower -2	695.407	1.3
		ITMy	Higher -2	695.471	1.1
	10/28/2005	ETMx	Lower -3	1030.54	1.4
		ETMx	Higher -3	1032.57	3.6
		ETMy	Lower -3	1034.45	2.6
		ETMy	Higher -3	1034.79	1.8
		ITMx	Lower -3	1041.61	2.0
		ITMx	Higher -3	1042.10	9.8
		ITMy	Lower -3	1043.31	2.6
		ITMy	Higher -3	1043.43	4.4
LHO 2K	1/26/2005 14:08	ETMy	Lower -1	343.747	6.7
		ETMx	Lower -1	343.812	1.1
		ETMx	Higher -1	344.046	1.3
		ETMy	Higher -1	344.086	1.5
		ITMx	Lower -1	348.938	4.5
		ITMy	Lower -1	349.194	2.6
		ITMy	Lower -1	349.235	1.0
		ITMx	Higher -1	349.452	1.5
	1/28/2005 10:00	ETMy	Lower -1	343.748	1.9
		ETMx	Lower -1	343.809	1.3
		ETMx	Higher -1	344.045	6.2
		ETMy	Higher -1	344.085	0.67
		ITMx	Lower -1	348.938	5.4
		ITMy	Lower -1	349.194	1.0
		ITMy	Higher -1	349.238	0.48

		ITMx	Higher -1	349.452	8.0
	1/26/2005 14:08	ETMy	Lower -2	687.435	1.2
		ETMx	Lower -2	687.663	1.0
		ETMx	Higher -2	688.172	1.1
		ETMy	Higher -2	688.213	7.8
		ITMx	Lower -2	697.903	5.6
		ITMy	Lower -2	698.443	2.1
		ITMy	Higher -2	698.553	3.0
		ITMx	Higher -2	698.957	1.6
	1/28/2005 10:00	ETMy	Lower -2	687.432	0.76
		ETMx	Lower -2	687.663	0.81
		ETMx	Higher -2	688.170	1.9
		ETMy	Higher -2	688.213	2.6
		ITMx	Lower -2	697.903	1.1
		ITMy	Lower -2	698.444	1.3
		ITMy	Lower -2	698.553	1.2
		ITMx	Higher -2	698.958	0.55
	1/26/2005 14:08	ETMy	Lower -3	1031.35	1.8
		ETMx	Lower -3	1031.62	2.3
		ETMx	Higher -3	1032.43	1.0
		ETMy	Higher -3	1032.54	4.2
		ITMx	Lower -3	1047.05	2.9
		ITMy	Lower -3	1047.82	3.4
		ITMy	Lower -3	1048.01	1.7
		ITMx	Higher -3	1048.61	2.3
	1/28/2005 10:00	ETMy	Lower -3	1031.35	2.5
		ETMx	Lower -3	1031.62	5.4

		ETMx	Higher -3	1032.43	6.7
		ETMy	Higher -3	1032.54	1.5
		ITMx	Lower -3	1047.05	3.2
		ITMy	Lower -3	1047.82	1.6
		ITMy	Higher -3	1048.01	2.2
		ITMx	Higher -3	1048.61	2.7

Table 3: Time domain violin mode Q measurements at the LIGO sites. Error bars are typically about 5% for these Q's.

Interferometer	Lock Stretch	Mirror	Mode	Frequency (Hz)	Q (X 10^5)	Notes
LLO	3/15/2004	ITMy	Lower -1	346.917	1.112	
		ITMy	Higher -1	346.968	1.133	
		ETMy	Lower -1	343.480	1.22	Controlled
		ETMy	Lower -1	343.480	1.226	Controlled
		ETMy	Higher - 1	344.421	1.22	Controlled
		ETMx	Higher – 1	343.656	0.397	Controlled
		ETMx	Higher -1	343.656	0.433	Controlled
		ETMx	Lower -1	343.092	0.488	Controlled
		ETMx	Lower -1	343.089	0.577	
		ETMx	Higher -1	343.654	0.862	
		ITMx	Lower -1	346.650	1.19	
		ITMx	Higher -1	347.038	1.65	
		ITMx	Higher -1	347.038	1.40	
		ITMx	Higher -2	694.088	1.62	
LHO 2K	1/29/2005	ITMx	Lower -1	348.938	0.86	1 W P_{in}
		ITMy	Lower -1	349.194	0.84	1 W P_{in}

		ITMy	Higher -1	349.236	0.90	1 W P_{in}
		ITMy	Higher -1	349.236	0.96	1 W P_{in}
		ITMy	Lower -1	349.194	0.87	1 W P_{in}
		ITMy	Lower -1	349.194	0.91	1 W P_{in}
		ITMy	Higher -1	349.236	0.95	
		ITMx	Lower -1	348.938	1.56	
		ITMx	Lower -1	348.938	1.56	
		ITMx	Higher -1	349.452	1.38	
		ITMx	Higher -1	349.452	1.38	
		ITMx	Lower -1	349.452	1.37	
		ITMy	Lower -3	1047.82	2.15	
		ITMy	Lower -3	1047.82	2.09	
		ITMy	Lower -3	1047.82	2.09	
		ITMy	Higher -3	1048.01	2.61	
		ITMy	Higher -3	1048.01	2.25	
		ITMy	Higher -3	1048.01	2.31	
		ITMx	Lower -3	1047.045	2.17	
		ITMx	Lower -3	1047.045	2.15	
		ITMx	Lower -3	1047.045	2.12	
		ITMx	Lower -2	697.903	1.47	
		ITMx	Lower -2	697.903	1.56	
		ITMx	Lower -2	697.903	1.51	
		ITMx	Higher -2	698.958	0.496	
		ITMx	Higher -2	698.956	0.498	
		ITMx	Higher -2	698.956	0.505	
		ITMx	Higher -3	1048.612	2.15	
		ITMx	Higher -3	1048.612	2.25	
		ITMy	Lower -2	698.444	1.12	
		ITMy	Lower -2	698.444	1.13	
		ITMy	Lower -2	698.444	1.15	

		ITMy	Higher -2	698.553	1.14	
		ITMy	Higher -2	698.553	1.17	
		ITMy	Higher -2	698.553	1.18	
LLO	5/31/2005 20:00	ITMy	Lower -1	346.912	0.89	Michelson Lock
		ITMy	Higher -1	346.959	0.90	Michelson Lock
		ITMy	Higher -1	346.959	1.03	Michelson Lock
		ITMy	Higher -1	346.959	0.97	Michelson Lock
		ITMy	Lower -1	346.912	0.73	Michelson Lock
	5/31/2005 22:00	ITMy	Lower -1	346.912	0.67	Michelson Lock
		ITMy	Higher -1	346.959	0.85	Michelson Lock
		ITMy	Higher -1	346.959	1.0	Michelson Lock
	5/31/2005 1:00	ITMx	Lower -1	346.644	0.755	
	5/31/2005 1:40	ITMx	Lower -1	346.644	0.759	
		ITMx	Lower -1	346.644	0.758	
		ITMx	Lower -1	346.644	0.885	
		ITMx	Higher -1	347.034	0.838	
		ITMx	Higher -1	347.034	0.918	
		ITMx	Higher -1	347.034	0.778	
		ITMy	Lower -1	346.909	0.719	
LLO	6/2/2005 1:45	ITMx	Lower -1	346.650	0.240	
		ITMx	Lower -1	346.650	0.251	
		ITMx	Lower -1	346.650	0.251	

		ITMx	Higher -1	347.037	0.871	
	6/3/2005 2:20	ITMx	Higher -1	347.037	0.574	1.0 W MC_{req}
		ITMx	Higher -1	347.037	0.551	1.0 W MC_{req}
		ITMx	Higher -1	347.037	0.545	1.41 W MC_{req}
		ITMx	Higher -1	347.034	0.534	2.0 W MC_{req}
		ITMx	Higher -1	347.034	0.525	2.82 W MC_{req}
		ITMx	Higher -1	347.034	0.517	3.98 W MC_{req}
	6/3/2005 3:15	ITMx	Lower -1	346.642	0.920	1.0 W MC_{req}
		ITMx	Lower – 1	346.642	0.949	1.41 W MC_{req}
		ITMx	Lower -1	346.642	0.926	2.00 W MC_{req}
		ITMx	Lower -1	346.642	0.919	2.82 W MC_{req}
		ITMx	Lower -1	346.642	0.907	3.98 W MC_{req}
		ITMx	Lower -1	346.642	0.933	3.98 W MC_{req} Moved +2 μm
		ITMx	Lower -1	346.642	0.937	3.98 W MC_{req} Moved +0.5 μm
		ITMx	Lower -1	346.642	0.934	3.98 W MC_{req} Moved -2.5 μm

		ITMx	Lower -1	346.642	0.950	3.98 W MC_{req} Moved +2.5 μm
		ITMx	Lower -1	346.642	0.940	3.98 W MC_{req} Moved +0.5 μm
		ITMx	Lower -1	346.642	0.962	2.82 W MC_{req}
		ITMx	Lower -1	346.642	0.973	2.00 W MC_{re}
		ITMx	Lower -1	346.642	0.941	1.41 W MC_{re}
		ITMx	Lower -1	346.642	0.964	1.00 W MC_{re}
		ITMx	Lower -1	346.642	0.986	1.41 W MC_{re}
		ITMx	Lower -1	346.642	0.950	2.00 W MC_{re}
		ITMx	Lower -1	346.642	0.943	2.82 W MC_{re}
		ITMx	Lower -1	346.642	0.928	3.98 W MC_{re}
LHO 4K	6/24/2005?	ITMx	Lower -1	347.174	0.94	
		ITMx	2	695.275	1.20	
		ITMx	3	1041.62	0.30	
LLO	5/16/2006	ITMx	Higher -1	347.038	1.25	Full Lock
		ITMx	Higher -1	347.038	1.28	Michelson Lock
		ITMx	Higher -1	347.038	1.38	Michelson Lock after alignment
LHO 4K	4/5/2006	ETMx	Lower -1	343.41	1.3	
	4/7/2006	ETMx	Lower -1	343.4	0.98	Non-

						exponential decay
		ETMx	Higher -1	344.1	0.96	
		ITMx	Lower -1	347.3	1.23	
		ITMx	Higher -1	347.5	1.23	
		ETMy	Lower -1	344.7	1.16	
		ETMx	Higher -1	344.8	1.21	

Table 4. Violin mode Q's from MIT test setup using a pre-used conventional clamps.

Date	Mode	Frequency (Hz)	Q (X 10^5)
2/28/06 – 3/3/06	Left 1	339.8	0.71
	Left 2	679.7	1.28
	Left 3	1019.7	1.01
	Left 4	1359.984	1.55
	Left 5	1700.34	1.12
	Right 1	338.986	0.83
	Right 2	677.978	1.26
	Right 3	1017.177	1.60
3/9/06 – 3/16/06	Right 1 LR	338.875	0.735
	Right 2 LR	677.783	0.994
	Right 3 LR	1016.860	1.12
	Right 4 LR	1356.108	1.15
	Right 5 LR	1695.739	1.46
	Right 1 FB	338.992	0.80
	Right 2 FB	677.994	1.33
	Right 3 FB	1017.172	1.40
	Right 4 FB	1356.530	1.54
	Right 5 FB	1696.262	1.77
	Left 1 LR	339.667	0.816
	Left 2 LR	679.398	1.42

	Left 3 LR	1019.289	1.08
	Left 5 LR	1699.719	1.20
	Left 1 FB	339.820	0.739
	Left 2 FB	679.703	1.39
	Left 3 FB	1019.742	1.06
	Left 4 FB	1360.0	1.70
	Left 5 FB	1700.492	1.43
4/13/06-4/24/06	Left 1 FB	338.35	0.609
	Left 2 FB	676.54	0.651
	Left 3 FB	1014.93	0.798
	Left 4 FB	1353.56	1.29
	Left 1 LR	338.21	0.524
	Left 2 LR	676.52	0.634
	Left 3 LR	1014.93	0.732
	Left 4 LR	1353.519	0.790
	Left 5 LR	1692.46	0.793
	Right 1 FB	336.33	0.699
	Right 2 FB	672.72	1.06
	Right 3 FB	1009.18	1.10
	Right 4 FB	1345.984	1.15
	Right 5 FB	1683.0	1.25

Table y. Violin mode Q's from MIT test setup using a conventional clamps directly after having been machined. Torque tightening the screws holding the clamp together was also controlled.

Date	Mode	Frequency	Q	Torque
6/20/06-6/23/06	Right 1 LR	334.547	1.12	0.71 N m
	Right 3 LR	1004.016	1.67	
	Right 5 LR	1674.003	1.79	
	Left 1 FB	336.906	0.860	
	Left 3 FB	1010.906	1.29	

	Left 5 FB	1685.688	1.61	
	Left 1 LR	336.766	0.860	
	Left 2 LR	674.5	1.04	
	Left 3 LR	1010.538	1.24	
	Left 5 LR	1685.078	1.54	
	Right 1 FB	334.672	1.10	
	Right 3 FB	1004.354	1.72	
	Right 4 FB	1339.469	1.82	
6/28/06 – 6/30/06	Right 1 LR	334.563	1.12	4.1 N m
	Right 2 LR	669.25	1.44	
	Right 3 LR	1004.077	1.62	
	Right 4 LR	1339.078	2.19	
	Right 5 LR	1674.203	1.97	
	Right 6 LR	2009.614	2.11	
	Left 1 LR	336.844	0.851	
	Left 2 LR	673.5	1.21	
	Left 3 LR	1010.431	1.39	
	Left 4 LR	1347.469	1.38	
	Left 5 LR	1684.987	1.55	
	Left 6 LR	2022.672	1.56	
	Left 7 LR	2360.781	1.55	
	Right 1 FB	334.703	0.931	
	Right 2 FB	669.484	1.49	
	Right 3 FB	1004.078	1.44	
	Right 4 FB	1339.547	1.65	
	Right 5 FB	1674.890	1.83	
	Right 6 FB	2010.565	1.77	
	Left 1 FB	336.875	0.81	
	Left 2 FB	673.688	1.07	
	Left 3 FB	1010.813	1.21	

	Left 4 FB	1347.922	1.31	
	Left 5 FB	1685.531	1.49	
	Left 6 FB	2023.391	1.80	
7/6/06-7/10/06	Left 1 FB	336.891	0.947	Max Torque (~ 5 N m)
	Left 2 FB	673.75	1.24	
	Left 3 FB	1010.891	1.26	
	Left 4 FB	1348.069	1.45	
	Left 5 FB	1685.656	1.48	
	Left 6 FB	2023.531	1.62	
	Left 7 FB	2361.781	1.87	
	Left 1 LR	336.797	0.928	
	Left 2 LR	673.547	1.27	
	Left 3 LR	1010.578	1.26	
	Left 4 LR	1347.609	1.44	
	Left 5 LR	1685.141	1.47	
	Left 6 LR	2022.891	1.50	
	Right 1 FB	334.733	0.985	
	Right 3 FB	1004.516	1.38	
	Right 5 LR	1675.047	1.69	
	Right 1 LR	334.625	0.996	
	Right 2 LR	669.328	1.30	
	Right 3 LR	1004.219	1.38	
	Right 5 LR	1674.406	1.54	

Table z. Violin mode Q's from MIT test setup using a DNA Collet to hold the wires at the top. Note that the modal frequencies have shifted slightly because the wire has a different length than with the conventional clamps.

Date	Mode	Frequency (Hz)	Q (X 10^5)
7/26/06	Left 1 LR	408.516	0.437
	Left 2 LR	817.203	0.883
	Left 3 LR	1226.065	0.578
	Right 1 LR	407.531	0.299
	Right 2 LR	815.156	0.934
	Right 3 LR	1223.031	0.732
	Right 1 FB	407.594	0.610
	Right 2 FB	815.266	1.04
	Right 3 FB	1223.203	1.15
	Left 1 FB	408.583	0.331
	Left 2 FB	817.286	0.919
	Left 3 FB	1226.221	1.06
7/27/06	Left 1 LR	409.000	0.398
	Left 2 LR	818.137	0.786
	Left 3 LR	1227.500	0.404
	Right 1 LR	407.531	0.428
	Right 2 LR	815.141	1.06
	Right 3 LR	1223.0	0.852
	Right 1 FB	407.609	0.521
	Right 2 FB	815.297	0.872
	Right 3 FB	1223.0	1.04
	Left 1 FB	409.087	0.548
	Left 2 FB	818.309	0.677
	Left 3 FB	1227.747	0.814

Table a. Violin mode Q's from MIT test setup using a Virgo inspired clamp with tool steel inserts at the clamping points. These inserts were pitted during cleaning with Liquinox and sanded down.

Date	Mode	Frequency (Hz)	Q (X 10^5)
1/12/07-1/22/07	Left 1 FB	348.468	0.554
	Left 2 FB	697.003	0.864
	Left 3 FB	1045.688	0.937
	Left 4 FB	1394.625	0.594
	Left 5 FB	1743.831	0.990
	Left 6 FB	2093.48	1.30
	Left 7 FB	2443.497	1.25
	Left 10 FB	3497.1	1.39
	Left 1 LR	348.461	0.656
	Left 2 LR	697.004	0.871
	Left 3 LR	1045.688	0.898
	Left 5 LR	1743.822	0.970
	Left 6 LR	2093.5	1.22
	Left 7 LR	2443.47	1.32
	Left 9 LR	3145.4	1.18
	Right 1 LR	344.016	0.525
	Right 2 LR	688.117	0.747
	Right 3 LR	1032.34	0.998
	Right 5 LR	1721.5	0.991
	Right 6 LR	2066.6	2.16
	Right 7 LR	2412.1	0.893
	Right 1 FB	344.02	0.625
	Right 2 FB	688.375	1.38
	Right 7 FB	2412.9	1.78

Table b. Violin mode Q's from MIT test setup using a pre-used conventional clamp with glue holding the wire to the standoffs. The left wire was held with commercial Krazy Glue and the right wire with Vac Seal.

Date	Mode	Frequency (Hz)	Q (X 10^5)
2/9/07-2/13/07	Right 1 LR	352.516	0.338
	Right 2 LR	705.109	0.188
	Right 3 LR	1057.867	0.705
	Right 5 LR	1764.5	0.456
	Right 1 FB	352.300	1.37
	Left 1 FB	339.375	0.252
	Left 2 FB	678.862	0.241
	Left 3 FB	1018.519	0.289
	Left 4 FB	1358.438	0.339
	Left 5 FB	1698.656	0.322